

# Epoxy/montmorillonite nanocomposites: influence of organophilic treatment on reactivity, morphology and fracture properties

Loïc Le Pluart<sup>a,\*</sup>, Jannick Duchet<sup>b</sup>, Henry Sautereau<sup>b</sup>

<sup>a</sup> *Laboratoire de Chimie Moléculaire et Thioorganique, UMR CNRS 6507 ENSICAEN-Université, 6, bd du Maréchal Juin 14050 Caen, Cedex, France*

<sup>b</sup> *Laboratoire des Matériaux Macromoléculaires, UMR CNRS 5627 Institut National des Sciences Appliquées-Bat. Jules Verne, 20 avenue Albert Einstein 69621 Villeurbanne, Cedex, France*

Received 28 February 2005; received in revised form 28 September 2005; accepted 17 October 2005

Available online 14 November 2005

## Abstract

Two different alkylammonium modified montmorillonites have been dispersed in epoxy network precursors in order to study the influence of the organophilic treatment on the reactivity and cure behavior of the networks, on the morphology of the final composites and on their elastic and fracture properties. An increase in the interplatelet distance during curing of the network (in addition to the initial swelling by the network precursors) is possible when the competition between cure kinetics, diffusion kinetics and interactions between network precursors and organophilic montmorillonite allows it. Network structure is not modified and a catalytic effect of the organoclays has been demonstrated. Correlation between morphologies and mechanical properties reveals that exfoliated nanocomposites lead to interesting stiffness improvements. However, intercalated nanostructures can lead to very interesting stiffness/toughness balance for glassy epoxy networks without lowering their glass transition temperature. This suggests that stiffness and toughness improvements might not be ruled by the same kind of morphologies. © 2005 Elsevier Ltd. All rights reserved.

**Keywords:** Epoxy/clay nanocomposites; Morphology; Fracture properties

## 1. Introduction

Polymer layered silicate nanocomposites are a new class of materials obtained by the dispersion of very high aspect ratio clay-type particles in a polymeric matrix. Montmorillonite is the layered silicate which has been the most widely used in polymeric matrixes due to its very interesting multiscale organization. It is made of platelets of one nanometer thick for several hundred nanometers long and wide. These platelets are stacked face to face in primary particles which are themselves grouped into aggregates. Obtaining a homogeneous dispersion of these very high aspect ratio nanometric platelets in a polymer should lead to interesting improvements in mechanical, thermal and barrier properties of the polymer for very low amounts of inorganic filler.

The first interesting results in this field were obtained in 1990's by the Toyota research group [1,2] which considerably improved mechanical performances of polyamide 6 with alkylammonium modified montmorillonite. From these first

results numerous studies have been performed with different polymers [3], more or less successfully improving the understanding of the behaviour of this new class of materials and revealing the difficulty of reaching the exfoliated state.

In situ polymerization of monomers has historically been the first way explored to obtain exfoliated nanocomposites. It has been initiated with the synthesis of polyamides and led to promising results especially in terms of tensile and impact properties at low filling rates [4]. This way of processing opened the possibility of very creative projects such as the use of functionalized alkylammonium ions leading to polymerization starting from clay surfaces or the grafting of metallocenes on the silicate surface which allowed synthesizing polyolefins within the galleries [5]. Modification of the silicate layer to make it compatible with the polymer matrix is a first step which cannot be neglected. The main technique used is the cationic exchange which takes advantage of the charge deficit of montmorillonite, to substitute the inorganic cations initially present on the layer surfaces by some long chain organic cations, generally alkylammonium. The efficiency of this modification on the ability of the clay to be exfoliated in polymers or in monomers has not been clearly established, since the behaviour of organoclay in an organic medium [6–8] is still not fully understood. It is however, well known that

\* Corresponding author. Tel.: +33 231 45 2842; fax: +33 231 45 2877.  
E-mail address: [loic.le\\_pluart@ensicaen.fr](mailto:loic.le_pluart@ensicaen.fr) (L. Le Pluart).

chain length [9] and functionality [10] play a capital role in the nanocomposite final morphology, but it has been demonstrated that the quantity grafted is a key parameter in organoclay structure as well [11–13].

Since, we are studying epoxy thermoset nanocomposites, it is necessary to use the in situ polymerization process; this is why organoclay swelling by monomers will be of great importance. In previous studies performed with epoxy monomers and diamine curing agents, it has been demonstrated that the organoclay and the curing agent used influence the morphology or the mechanical properties [3,14–23] but few studies deal with the role played by the initial state of dispersion in the reactive mixture, curing cycle or polymerization kinetics [24,25]. Moreover, there is no clear trend linking structure to properties on these materials, since for instance the effect of organoclay exfoliation on thermoset glass transition temperature can vary from one study to another [14–16].

With this study we want to get a better understanding of how the chemical interactions between a modified montmorillonite and polymer network precursors rule the state of dispersion in the reactive mixture, the final architecture of the nanocomposites and their mechanical properties. In order to obtain ‘interaction induced architectures’ we did not use any shearing during the nanocomposite processing. To vary the interactions we used two different curing agents and two montmorillonites modified with different alkylammonium ions having, however, the same chain length. One of the alkylammonium has an aliphatic 18 carbon atom chain, the other one has an additional benzyl group on its nitrogen atom. Concerning the curing agents, one is a rigid aromatic diamine, the other one is a long aliphatic diamine. With these combinations we obtain different interactions in the reactive mixture, different polymerization kinetics, and different solid state properties.

In order to be sure that variations in the properties of the epoxy/amine systems are due to the montmorillonite dispersion, we studied carefully the influence of organoclay on epoxy/amine network formation by kinetic experiments. The influence of network formation on the dispersion at the nanometer and micrometer scale levels was also studied with in situ SAXS measurements using synchrotron radiation. The final architecture of the nanocomposites was characterized using transmission electron microscopy. We tried to link the differences observed in the state of dispersion and in its evolution to the interactions between organoclays and monomers. In addition, the architecture of the nanocomposites will be connected to stiffness, strength and toughness of the networks, allowing a better understanding of how interactions govern properties.

## 2. Experimental

### 2.1. Materials

Two alkyl ammonium-modified montmorillonites have been used in this study. Commercial organoclay Tixogel MP250 is a benzyl dimethyl tallow alkyl ammonium

montmorillonite. It has been supplied by Société française des Bentonites et Dérivés. Interlayer distance (further noted  $d$ -spacing or  $d_{001}$ ) determined by X-ray diffraction is 20.2 Å. Home-modified OPTC18 is an octadecylammonium ion modified montmorillonite which has been elaborated in large quantities (100 g) from a sodic montmorillonite by cationic exchange as described earlier [26].

The epoxy prepolymer is the diglycidyl ether of bisphenol A, ( $\bar{n}$  = 0.15) (LY556, Vantico), further noted DGEBA. The first curing agent is an aliphatic diamine with a polyoxypropylene backbone (Jeffamine D2000, Hunstman, further noted D2000). It leads to an elastomeric network with a sub ambient  $T_g$  of  $-59$  °C when mixed in stoichiometric ratio with DGEBA. The other curing agent is the 4,4'-methylenebis[3-chloro-2,6-diethylaniline] (further noted MCDEA). It is a short aromatic diamine, which leads after stoichiometric reaction with the epoxy prepolymer to a thermoset network with a high  $T_g$  of 177 °C [27].

Curing of the DGEBA/D2000 system is performed for 4 h at 80 °C followed by 3 h at 125 °C. Concerning the DGEBA/MCDEA reactive mixture, the curing is composed of one step of 7 h at 135 °C and 2 h at 200 °C. The curing cycle applied to the nanocomposites is the same as the one of the corresponding matrix.

All nanocomposite filling rates are expressed in grams of organoclay per 100 g of total resin (phr). One should note that the real amount of inorganic material is inferior to this rate due to the presence of the organic modifier (around 30% in weight as revealed by TGA analyses). The dispersion of organoclay in the monomers is performed manually, without additional shearing, to be able to observe interaction-induced morphologies, and then the reactive mixtures are poured into PTFE molds, screwed between two plates and cured in an oven.

### 2.2. Characterization

Gel times of the epoxy/amine systems with or without organoclay have been determined at the isofrequency crossover point of the  $\tan \delta$  curves during isothermal curing in a dynamic rheological analysis device RDAII from Rheometric Scientific with plate/plate geometry using 40 mm wide plates (Fig. 1). This method of determining the gel point is very accurate, since it is based on the experimental demonstration of the power-law relaxation behavior of critical gels [28,29].

The measurement of the glass transition temperature of DGEBA/MCDEA samples has been performed by DSC at 10 °C/min under argon circulation. The device used is a Mettler Toledo DSC 30. Conversion during isothermal curing of the DGEBA/MCDEA system has been calculated using the equation of Di Benedetto modified by Pascault and Williams [30].

It is impossible to apply the same method to the DGEBA/D2000 system because its glass transition temperature varies from  $-70$  °C before reaction to  $-59$  °C for a completely crosslinked network. In this case, conversion has been determined by measuring the disappearance of the

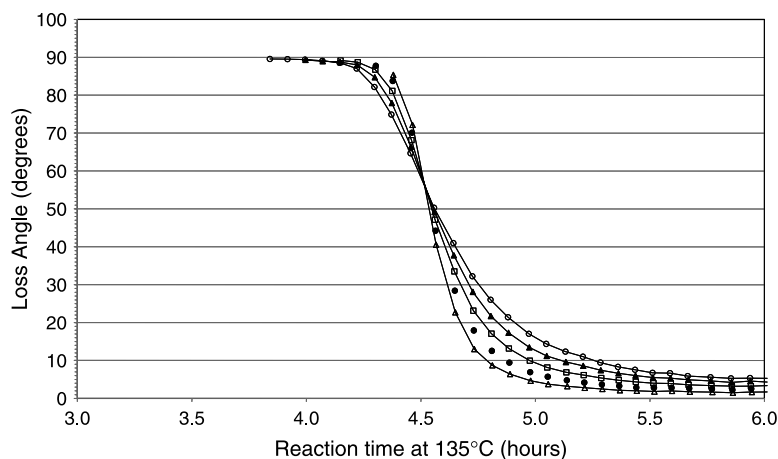


Fig. 1. Loss angle evolution around the gel point for the neat DGEBA/MCDEA system as a function of isothermal curing time at 135 °C. Frequency varies from 0.1 (empty triangles) to 100 rad s<sup>-1</sup> (empty squares).

DGEBA peak with a waters steric exclusion chromatography device [31]. This device is composed of 4 Styragel columns of 1000, 500, 200 and 50 Å and two detectors (refractometer and UV).

Interplatelet distance measurements have been measured by X-ray diffraction on a Siemens D500 with a copper anode, working with a 20 kV tension and 30 mA intensity. Tests have been performed on suspensions of organoclay in the monomers submitted to isothermal reaction over various times in order to evaluate the evolution of the *d*-spacing during curing of the epoxy/amine systems. Some in situ measurements were also carried out using small angle X-ray diffraction during isothermal curing of the sample on the D27 synchrotron line of the LURE at Orsay.

The morphology of the obtained nanocomposites has been observed by transmission electron microscopy with a Phillips CM120 microscope. Samples have been prepared using an ultramicrotome at room temperature for high-*T<sub>g</sub>* samples and at -70 °C for rubbery samples.

The mechanical properties have been measured at 22 °C on a 2/M device from the MTS company. For the rubbery materials, at least five dog-bone H3 shaped samples (NFT 51-034) leading to a standard deviation inferior to 5% have been tested in tension with a 5 mm/min crosshead speed. The modulus has been calculated using the rubber elasticity theory. The work at failure has been recovered from strain and stresses at break in tension. Concerning the thermoset system, Young's modulus has been determined in tension with a 1 mm/min crosshead speed using Vishay Micro-measure strain gauges on at least five ISO 60 samples. The fracture properties of the thermoset system have been evaluated at 25 °C with the measurement of fracture toughness *K<sub>IC</sub>* on single edge notched samples in three points bending (6×12×48 mm<sup>3</sup>) at 10 mm/min according to Williams and Cawood method [32]. *K<sub>IC</sub>* is an average of at least 10 tests with a crack length on sample width ratio varying from 0.3 to 0.6.

### 3. Results and discussion

#### 3.1. Influence of the organoclay on the network formation

Mechanical properties of a nanocomposite are generally compared to those of the matrix. In order to ensure that changes in mechanical properties are due to organoclay dispersion, it is necessary to check that the presence of the organoclay does not modify the network chemical structure. Indeed any changes in network structure can modify the matrix properties and lead to erroneous conclusions.

Prior to characterizing network formation, we measured the temperature at the beginning of homopolymerization reaction of DGEBA in absence and in presence of organoclay. These temperatures have been determined by DSC during a dynamic scan performed at 5 K/min. As in the studies performed by Lan et al. [17] and Wang et al. [33], the temperature of the beginning of homopolymerization is decreased in the presence of organoclay (Table 1). Nevertheless, at the temperatures at which we perform the curing of the networks (80 and 135 °C), this reaction can be neglected.

Monitoring of the viscoelastic properties of DGEBA/MC-DEA based systems with a multifrequency test during isothermal curing at 135 °C reveals that gel time of this epoxy/amine system is decreased in presence of organoclay (Fig. 2). In order to highlight this we have shown only two of the five frequencies used during the multiwave characterization.

When these gel times are plotted on the curves of the evolution of conversion vs. isothermal time of curing (Fig. 3),

Table 1  
DGEBA's homopolymerization starting temperature in presence of various organoclays

Systems	DGEBA	DGEBA + 5 phr Tixogel	DGEBA + 5 phr OPTC18
DGEBA's homopolymeriza- tion starting temperature (°C)	350	310	200

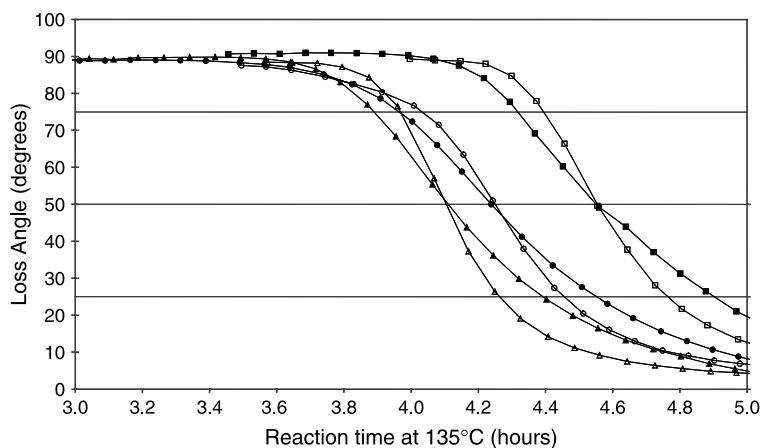


Fig. 2. Loss angle evolution vs. time of isothermal curing at 135 °C for neat DGEBA/MCDEA (squares), DGEBA/MCDEA + 5 phr Tixogel (circles) and DGEBA/MCDEA + 5 phr OPTC18 (triangles). Frequencies plotted are 10 (empty symbols) and 100  $\text{rad s}^{-1}$  (full symbols).

one can notice that the conversion at gel is not significantly modified by the presence of organoclay and corresponds to the value of 0.58 that can be calculated from Macosko–Miller theory [34].

These two observations lead to the conclusion that the organoclay does not modify strongly the reaction taking place between the epoxy and the amine, but only accelerates it. We can conclude from these experiments that organoclay has a catalytic effect on the DGEBA/MCDEA reaction. The catalytic power of the two different organoclays can not be significantly distinguished and linked to the chemical nature of the alkylammonium ions of the clay.

Concerning the DGEBA/D2000 system, gel time is decreased in the presence of Tixogel (curves *B* on Fig. 4) as with the DGEBA/MCDEA system. It is however, impossible to determine any gel time in presence of OPTC18 because the  $\tan \delta$  curves never cross over (curves *C* on Fig. 4). This very singular evolution of the viscoelastic properties of this reactive mixture has not been explained up to now. We can verify that this evolution is not due to chemical gelation. Indeed, as can be seen on the neat system curves (Fig. 4), when the gel point approaches,  $\tan \delta$  values determined at high frequencies are first affected and decrease before values measured with lower frequencies. In the presence of OPTC18,  $\tan \delta$  values measured at low frequency decrease first. The shape of the curves

resembles the one obtained during polymerization of thermoset/thermoplastic blends with reaction induced phase separation [35]. We think that for the system containing OPTC18, a physical phenomenon (which could be the formation of a physical gel due to organoclay exfoliation in the network precursors) prevents us from measuring the chemical gel point of this system by this method.

At any curing time,  $G'$  and  $G''$  vary with the pulsation following power laws of respective exponents  $n'$  and  $n''$ . The gel point is defined as the point where  $n' = n'' = \Delta$  [36]. The  $\Delta$  parameter is characteristic from the network structure. Introduction of Tixogel in the DGEBA/D2000 system does not affect the value of the  $\Delta$  parameter ( $\Delta = 0.75$  for the neat system and 0.78 with 5 phr Tixogel) which is another good indication of the fact that the network chemical structure is not affected by the presence of the organoclay. Moreover, this 0.7 value of  $\Delta$  is in good agreement with the literature concerning other epoxy/amine networks [36].

Nevertheless, gel times of the system containing the OPTC18 were determined using the insoluble fraction method. Samples reacted at 80 °C are dissolved in THF at 0 °C which stops the reaction by dilution and temperature effects. Then a SEC experiment is performed on the soluble fraction, to evaluate the conversion from the disappearance of the DGEBA monomer characteristic peak. Once again, we conclude that

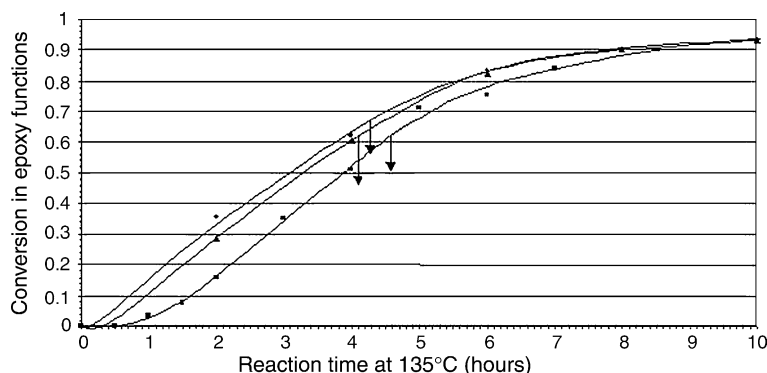


Fig. 3. Epoxy functions conversion vs. isothermal time of curing at 135 °C for neat DGEBA/MCDEA (squares), DGEBA/MCDEA + 5 phr Tixogel (triangles) and DGEBA/MCDEA + 5 phr OPTC18 (circles). Arrows indicate the gel time determined for each system.

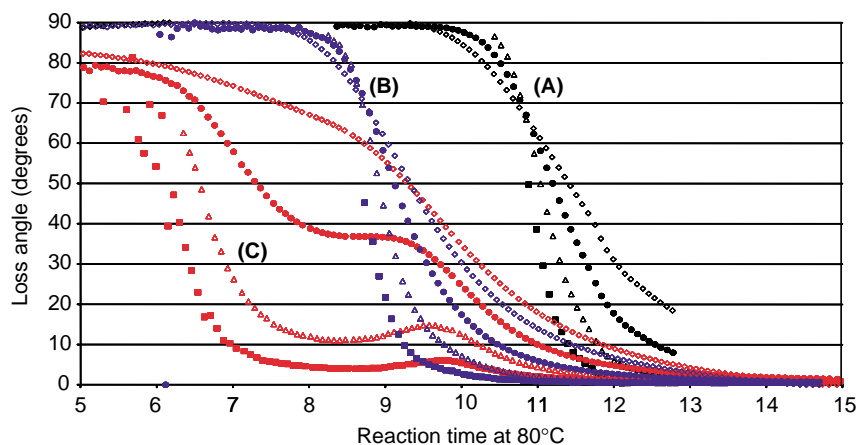


Fig. 4. Loss angle evolution vs. time of isothermal curing at 80 °C (frequencies 10 and 100  $\text{rad s}^{-1}$ ) for neat DGEBA/D2000 (A), DGEBA/D2000 + 5 phr Tixogel (B) and DGEBA/D2000 + 5 phr OPTC18 (C). Frequencies plotted are 0.1 (squares), 1 (triangles), 10 (circles) and 100 (diamonds).

organoclay catalyses the epoxy/amine reaction for the system with Tixogel, since gel time is decreased but conversion at gel still corresponds to the theoretical value (Fig. 5). For the system containing the OPTC18 organoclay, the conversion at the gel time seems to be slightly higher than this theoretical value.

Two possibilities were examined to explain this last observation. First it has been suggested that OPTC18 catalyzes the DGEBA homopolymerization reaction. However, this change in conversion at the gel point would have been observed with the DGEBA/MCDEA system as well, since it is polymerized at higher temperatures. The second possibility could be the presence of physisorbed octadecylamines on the OPTC18 organoclay surface, which would participate in the reaction and cause a change in the stoichiometry. However, since we introduce only 5 phr of organoclay, even if all the physisorbed material (evaluated earlier as 19.5% of the organoclay mass [37]) were monoamines participating in the reaction the conversion at the gel point wouldn't be increased in such a way.

Finally, we suppose that this phenomenon might be due to an exceptional state of dispersion of this organoclay in this

system which has been highlighted by SAXS measurements as will be stated later. This good dispersion might lead to the impossibility of completely extracting the unreacted epoxy monomers and consequently to the measurement of a lower monomer concentration in the extracted fraction and of an increased conversion.

The glass transition temperature of both networks is not affected after full curing of the samples, which is another good indication that the network structure is not affected by organoclay presence and that it has only a catalytic effect. We insist on the term 'full curing', since in some studies which observe a decrease in  $T_g$  of the system, it might be attributed to the barrier effect of organoclay, preventing monomers to diffuse and react. For instance nanocomposites synthesized by Kornmann et al. [16], curing is performed 30° under the infinite glass transition temperature of the DGEBA/3DCM network. Thus, once the  $T_g$  of the network has reached the curing temperature, the crosslinking reaction is performed in the glassy state, ruled by diffusion phenomena and therefore, completion of crosslinking cannot be reached. This should be taken into account in addition to the degradation of alkylammonium ions which is proposed. The absence of this

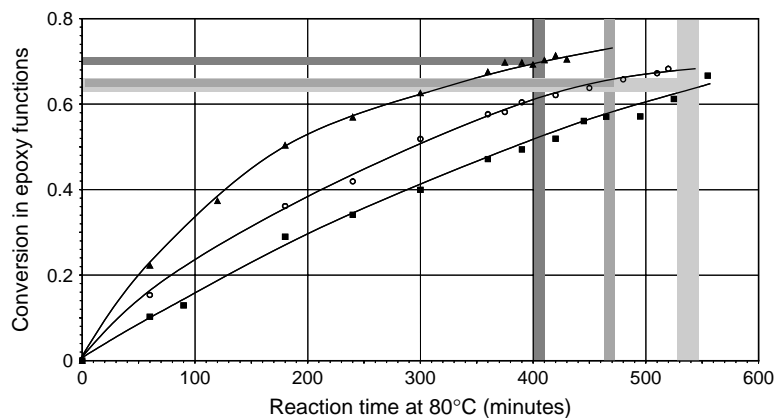


Fig. 5. Epoxy functions conversion vs. isothermal time of curing at 80 °C for neat DGEBA/D2000 (squares), DGEBA/D2000 + 5 phr Tixogel (circles) and DGEBA/D2000 + 5 phr OPTC18 (triangles). Grey bars represent the gel time measured from insoluble method and the corresponding estimated conversion at gel (light grey: neat system, medium grey: with 5 phr Tixogel, dark grey: with 5 phr OPTC18).

Table 2  
*d*-Spacing of Tixogel at 5 phr in epoxy/amine systems at the beginning and at the end of polymerization

Epoxy system + 5 phr Tixogel	DGEBA/MCDEA	DGEBA/D2000
<i>d</i> -Spacing when reaction starts (Å)	33.2	33.7
<i>d</i> -Spacing at end of the reaction (Å)	33.9	35.0

decrease in  $T_g$  with DGEBA/D230 system should be linked with the post curing step they perform above the infinite glass transition temperature of the system.

However, in our case, the use of a long curing schedule above  $T_g$ , systematic post curing above the infinite glass transition temperature, and absence of residual reaction enthalpy should ensure that this non-evolution of  $T_g$  can be attributed to the lack of effect of organoclay on the network structure. Similarly, Lee et al. [14] did not observe any effect on  $T_g$  of thermoset systems. Since, organoclays used in this work do not affect the network structure in both cases, we will be able to discuss the mechanical properties of nanocomposites, without having any matrix modifications to consider.

### 3.2. Influence of network formation on organoclay dispersion

Evaluating the evolution of the dispersion at the nanometer scale by means of XRD *d*-spacing measurement can give good information on the eventual influence of the network formation on the state of dispersion of the organoclay. Observation of the evolution of the dispersion at the micrometer scale is quite difficult in the case of reactive systems changing from a liquid state to a solid one. However, we described earlier [26] that the quality of the dispersion at the nanometer and at the micrometer level in the monomers of these systems seems to be linked together when no additional shear is applied during the process.

Concerning the systems containing Tixogel, we can notice in Table 2 that at the beginning of the reaction both reactive mixtures have swelled the organoclay, since the *d*-spacing has

been increased from 20.2 up to 34 Å. This increase in the *d*-spacing is linked to good interactions between the organoclay and its dispersion medium and demonstrates a good level of dispersion at the nanometer and micrometer scale levels [26].

During the isothermal reactions the *d*-spacing remains unchanged whatever the curing agent used, demonstrating that the polymerization of the epoxy/amine systems does not modify the Tixogel state of dispersion at the nanometer level (Fig. 6). In situ small angle X-ray scattering measurements (during curing for the DGEBA/D2000 system and on a cured sample for the DGEBA/MCDEA system) confirm that no peak appears at lower diffraction angle values confirming the non-evolution of the state of dispersion during the polymerization of these systems.

Concerning the systems containing OPTC18. The observations are very different.

In this case, the initial state of dispersion (before polymerization) is also good (Table 3), since both reactive mixtures swell the organoclay. One should notice that when OPTC18 is dispersed in the DGEBA/D2000 system, SAXS has to be used to measure the *d*-spacing of the clay even before polymerization, since the interplatelet distance (50–80 Å) is in this case out of the range of distances measurable using classical XRD (a reflexion peak prevents from detecting any reliable signal for  $2\theta$  situated between 0 and  $2^\circ$  in most cases). This confirms the necessity to use SAXS in order to avoid abusive conclusions. For instance, an exfoliated state of dispersion may be deduced from the absence of diffraction peak on a XRD spectrum whereas it can be due to the limits of this experimental device.

We can notice in Table 3 that with OPTC18, the *d*-spacing increases during isothermal reaction of both reactive mixtures. The *d*-spacing even reaches distances greater than 100 Å when OPTC18 is dispersed in the DGEBA/D2000 system.

This demonstrates the possibility of increasing the quality of dispersion at the nanometer scale during the polymerization of the network. It can also be noted that on the in situ SAXS

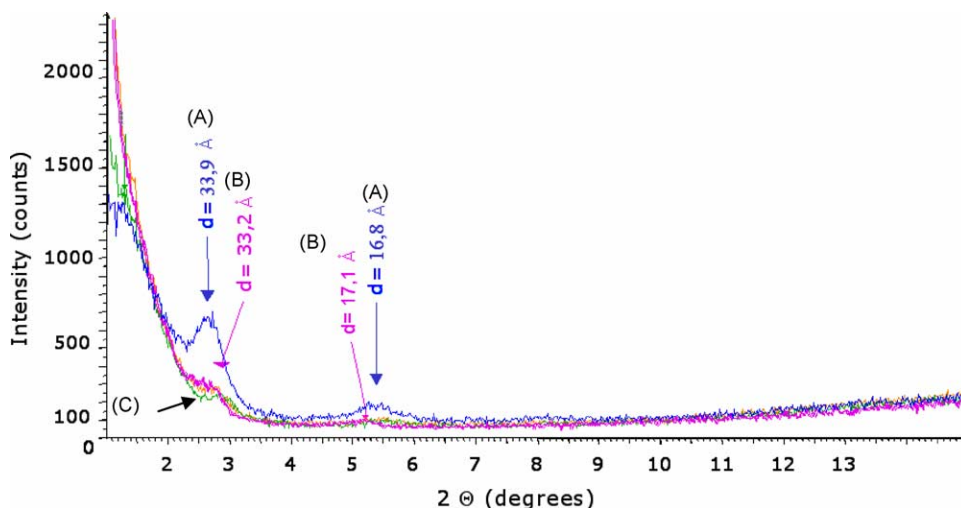


Fig. 6. XRD measurement of *d*-spacing evolution during polymerization of DGEBA/MCDEA + 5 phr Tixogel system: after 3 h at 135 °C (a), 5 h at 135 °C (b) and 7 h at 135 °C + 2 h at 200 °C (c).

Table 3  
*d*-Spacing of OPTC18 at 5 phr in epoxy/amine systems at the beginning and at the end of polymerization

Epoxy system + 5 phr OPTC18	DGEBA/MCDEA	DGEBA/D2000
<i>d</i> -Spacing when reaction starts (Å)	33.0	54.5
<i>d</i> -Spacing at end of the reaction (Å)	70	110

measurements realized with the DGEBA/D2000 system (Fig. 7) that as long as the duration of the isothermal polymerization increases (curves *a*–*d*), the intensity of the peak at 54.5 Å decreases until it disappears after 8 h at 80 °C, whereas the intensity of the peak around 110 Å increases continuously. If one considers now the spectrum obtained on a sample having been submitted to the curing cycle used for nanocomposites synthesis of 4 h at 80 °C and 3 h at 125 °C (curve *e*), one can see that both peaks are visible. We infer from this observation that when the chemical gelation of the reactive system occurs more quickly (with the nanocomposite curing cycle, it occurs during the first 20 min of the step at 125 °C) the state of dispersion seems to be frozen as already suggested by Brown et al. [18]. As a consequence, as long as gelation does not occur, the state of dispersion can evolve as can be seen during an isothermal polymerization at 80 °C (in this case gelation takes place after 10 h).

As a conclusion, we proved that the quality of the dispersion of organoclay can be improved by the polymerization of the epoxy network.

These improvements are not only due to the kind of organoclay used, since OPTC18 reaches very high *d*-spacings during DGEBA/D2000 polymerization and is less increased using DGEBA/MCDEA.

Nor are they only due to the epoxy system chosen, since the variation of the *d*-spacing is not the same for OPTC18 and Tixogel when they are dispersed in the DGEBA/D2000 system. The possibility of increasing the *d*-spacing is linked to interactions and chemical affinities between the organoclay and the network precursors as well as with reaction and diffusion kinetics of the reactive systems as generally proposed

[25]. For instance, with the DGEBA/MCDEA system, the gel point is reached more quickly than with DGEBA/D2000 and as a consequence the time available for species to diffuse is reduced. It can be one of the reasons why the interplatelet distance of OPTC18 is smaller when it is dispersed in the DGEBA/MCDEA system. Moreover, since the glass transition temperature of this reactive mixture increases when the reaction proceeds, it is always closer to the isothermal curing temperature than with DGEBA/D2000 (in this case  $T_g$  varies from –70 to 59 °C). This is responsible for a lower molecular mobility in the DGEBA/MCDEA reactive mixture and lower diffusion kinetics which prevent unreacted molecules to access the galleries.

So, it has been shown that *d*-spacings can or cannot be increased during the polymerization of an epoxy network as a function on epoxy system/organoclay interactions, polymerization and diffusion kinetics. Despite good swelling in the monomers, indicating good interactions with its dispersion medium, Tixogel presents a lower capacity to increase its *d*-spacing during network formation.

However, the mechanism responsible for an increase in the interplatelet distance has not been clearly identified yet and seems to be quite complex if one refers to the work on activation energies performed by Chen et al. [25]. It has been proposed that network formation from organoclay surfaces in the galleries is responsible for this phenomenon when certain conditions involving interlayer expansion activation energy, polymerization action energy, and diffusion kinetics are fulfilled. Knowing that networks are generally less dense than the monomers, other parameters than volume filling principle should be taken into account to justify this expansion such as solubility problems for instance (interaction parameter of the network is different from the one of the monomers and consequently interactions of the organoclay with its dispersion medium should evolve continuously during network formation).

Finally, these measures lead to another question: when can we consider an organoclay as exfoliated? Indeed one can really wonder whether an organoclay with an interplatelet distance

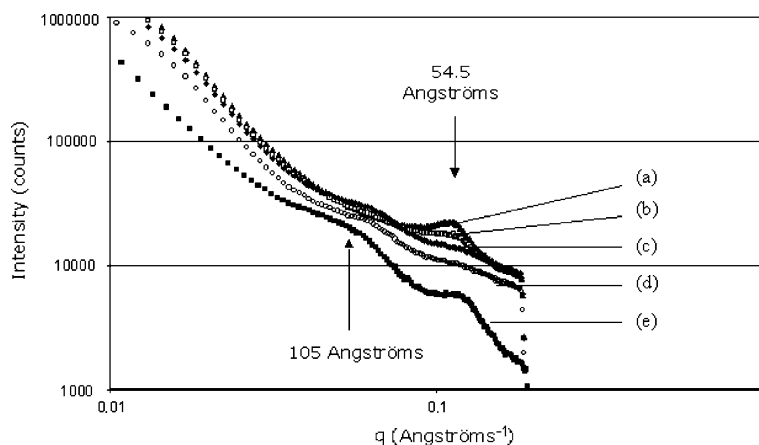


Fig. 7. SAXS measurement of *d*-spacing evolution during polymerization of DGEBA/D2000 + 5 phr OPTC18 system: after 35 min (a), 1 h (b), 3 h (c), 4 h at 80 °C (d) and 4 h at 80 °C + 3 h at 125 °C (e).

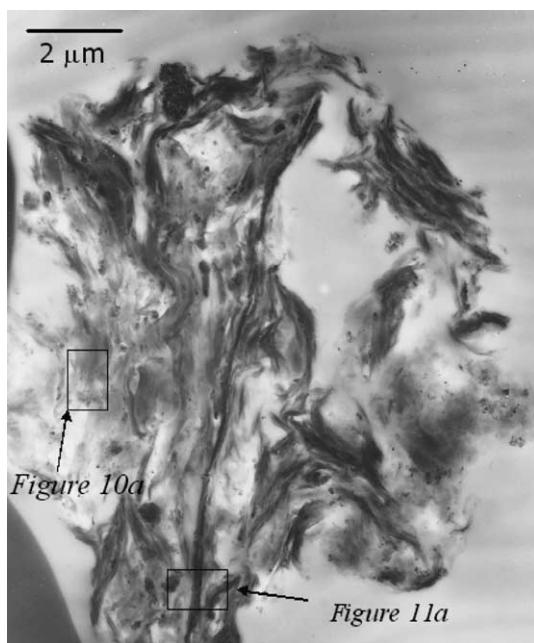


Fig. 8. TEM picture of DGEBA/D2000+5 phr Tixogel composite.

higher than 100 Å can still be considered as intercalated. It should not be forgotten that SAXS and WAXS inform us only on the structured part of the organoclay, and do not inform us about the eventual presence of truly exfoliated organoclay in the mixture.

This is why precise observations of the final morphologies at different scale levels are necessary to have an idea of the global state of dispersion.

### 3.3. Nanocomposite morphologies and mechanical properties

In this last part we will separate observations and measurements performed on the elastomeric DGEBA/D2000

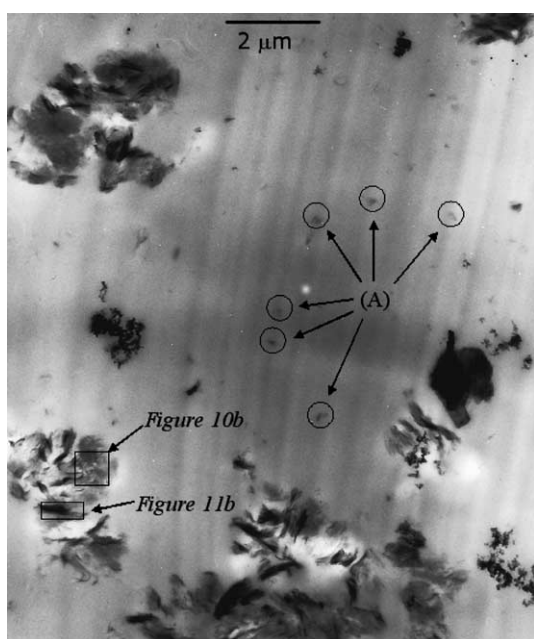


Fig. 9. TEM picture of DGEBA/D2000+5 phr OPTC18 composite.

and glassy DGEBA/MCDEA based nanocomposites. We characterized all the samples by TEM at different scale levels and measured some mechanical properties in terms of stiffness, strength and toughness. Our aim was to compare the morphologies, try to link them to the mechanical properties, and try to understand how these micro and nanomorphologies can affect macroscopic properties.

In the rubbery DGEBA/D2000 matrix, the states of dispersion of the two organoclays are completely different at the micrometer scale as can be seen in Figs. 8 and 9. We recall here that these two morphologies are interaction-guided morphologies and that no additional shear has been used during the process. Consequently chemical interactions between organoclay and its dispersion medium lead to different morphologies.

The Tixogel forms coarse aggregates up to 10 micrometers thick as can be seen in Fig. 8, whereas, OPTC18 (Fig. 9) is dispersed more finely. OPTC18 aggregates are smaller, more homogeneously dispersed in the matrix and one can also distinguish very small aggregates barely visible at this scale level (A in Fig. 9).

However, these aggregates have more or less the same sub-structure. Whatever the organoclay used, the aggregates are made of diffuse light grey and darker zones, which resemble some more or less dense parts of the aggregates.

Using a zoom to take a closer look at the light grey zones, no kind of ordering at the nanometer scale level is observed. This is verified with the two different organoclays as can be seen in Fig. 10. These zones look like exfoliated zones where the platelets are no longer parallel to each other. On the contrary the dark zones observed in the aggregates (Figs. 8 and 9) are intercalated zones as can be seen in Fig. 11. In these zones the platelets are clearly parallel to each other. The distances that can be measured on these TEM pictures correspond to the distances of 35 and 110 Å measured by XRD and SAXS for each one of the two organoclays.

The conclusion is that morphologies obtained by chemical interactions (no additional shear) have to be considered in their whole and not only at the nanometer scale. Indeed the main differences observed in the DGEBA/D2000 nanocomposites are at the micrometer level with a better dispersion of the OPTC18, whereas the inner structure of these aggregates is roughly the same with intercalated and exfoliated zones in both kinds of aggregates. OPTC18 has, however, a better dispersion at the nanometer level, since the *d*-spacing in its intercalated zones is much higher than the one of the Tixogel.

We used the rubber elasticity theory to calculate the shear modulus from tensile tests. We measured stress and strain at break as well as work at failure to evaluate the strength of these nanocomposites. All these mechanical properties are also compared with those of the matrix and of a composite realized with a hydrophilic nanosized fumed silica filler (Aerosil 200 from Degussa) introduced at the same ratio of 5 phr.

As can be seen in Table 4, the modulus is clearly increased by the presence of organoclay. Whatever the organoclay used this increase is always higher than 20%. Moreover, considering that in 5 phr of organoclay 30% of the mass is represented by



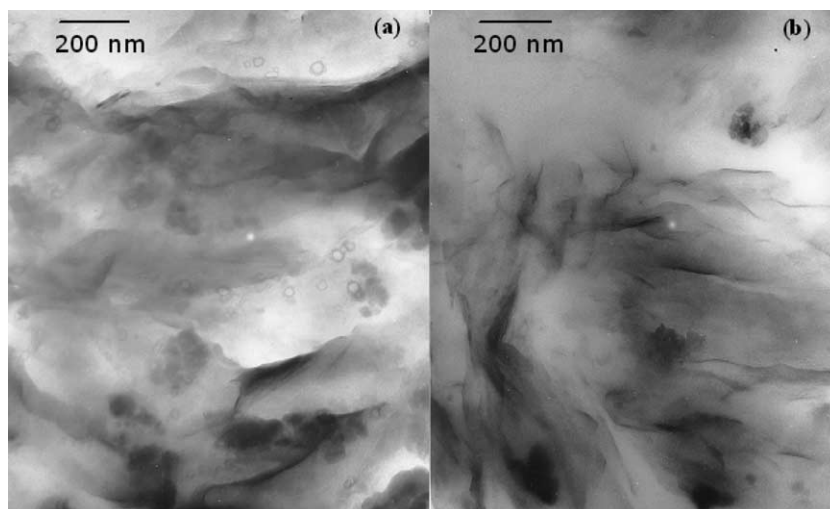


Fig. 10. TEM picture of exfoliated regions in DGEBA/D2000+5 phr Tixogel (a) and DGEBA/D2000+5 phr OPTC18 (b) composite.

the organic modifier, one can say that this increase in modulus is higher than the one obtained using a conventional filler like silica even without using shearing during the process.

One can verify that the presence of organoclay also has a reinforcing effect, since the stresses and strains at break are increased simultaneously as can be checked in Table 5. This leads to a great increase in the work at failure of this crosslinked rubbery epoxy system which can reach up to 500% with 10 phr of Tixogel.

As a conclusion, organoclay introduction leads to improvements in both stiffness and strength of this rubbery matrix. The increases observed are always higher than the ones obtained using a conventional filler. It is however, difficult to link these modifications of mechanical properties to the morphologies. The nanocomposite containing OPTC18 seems to have slightly higher mechanical properties than the one containing Tixogel and presents a better dispersion at the micrometer and at the nanometer scale levels. The observed differences might not be significant enough to link them with certainty.

With the DGEBA/MCDEA based nanocomposites the morphologies observed are completely different and the changes in the mechanical properties measured are very interesting as well. Young's modulus values obtained in

uniaxial tensile testing are shown in Table 6. One should notice the huge improvement in the modulus using 5 phr of Tixogel whereas OPTC18 does not increase the modulus significantly (as well as silica) in this high- $T_g$  thermoset matrix.

This notable difference between the two organoclays leads us to compare the morphologies of these nanocomposites. At the micrometer level, the states of dispersion of the two organoclays are completely different. Tixogel (Fig. 12) is organized in small, fine, quite dense and well dispersed aggregates. This unusual morphology (when compared to all the other ones observed at this scale level) should be related to the increase in the stiffness of the nanocomposite. On the other hand OPTC18 (Fig. 13) forms quite large aggregates (more or less 5  $\mu\text{m}$  in diameter). These seem to be less dense and more swollen by the matrix.

At the nanometer level (Fig. 14(a)), one can observe that Tixogel aggregates in the DGEBA/MCDEA matrix are made of few primary particles stacked together. One cannot observe any exfoliated zones in these nanocomposites. The primary particles are not significantly swollen by the matrix and the platelets are all parallel to each other with an interplatelet spacing of 35 Å corresponding to XRD measurements (Fig. 14(b)).

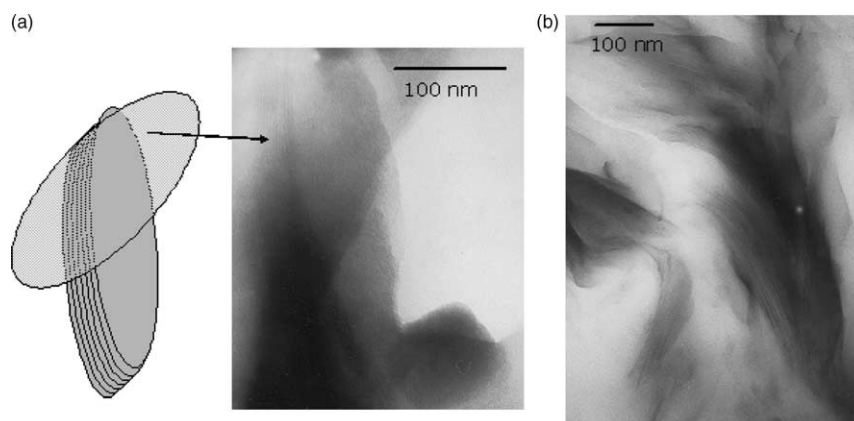


Fig. 11. TEM picture of intercalated regions in DGEBA/D2000+5 phr Tixogel (a) and DGEBA/D2000+5 phr OPTC18 (b) composite.

Table 4  
Shear modulus ( $G$ ) and relative modulus ( $G/G_0$ ) for DGEBA/D2000 based nanocomposites at 25 °C

DGEBA/D2000	Neat	+5 phr Tixogel	+10 phr Tixogel	+5 phr OPTC18	+5 phr Aerosil 200
$G$ (MPa)	0.50	0.61	0.82	0.65	0.66
$G/G_0$	1	1.22	1.64	1.30	1.32

The inner structure of the OPTC18 aggregates (Fig. 15(a)) is more complex. We can notice some hazy zones, which look like exfoliated zones. However, in other parts of the aggregate platelets are regularly intercalated by the matrix, and some isolated little groups of few platelets in the matrix are also visible (Fig. 15(b)). Despite this diversity, the dispersion of the OPTC18 platelets at the nanometer scale is clearly finer than those of Tixogel. In the intercalated zones one cannot distinguish the primary particles anymore but a zoom allows observing platelets facing each other regularly with a repetitive interplatelet distance (Fig. 15(c)). The global morphology of the OPTC18 could be described as ‘swollen’ at the micrometer as well as the nanometer scale level.

When linking these observations to the mechanical properties, we conclude that this last morphology is much less favorable to an increase in the modulus of the thermoset glassy matrix than the one presented by the Tixogel. This is surprising when compared to the results of Miyagawa et al. [23] who linked the increase in tensile modulus to an optimal dispersion at the nanometer scale and concluded that intercalated state of dispersion should give smaller modulus improvements. However, Boucard et al. [38] demonstrated on polypropylene/clay nanocomposites that nodules of intercalated platelets (obtained with a stearic maleic anhydride coupling agent) can lead to best stiffness improvements than a well dispersed morphology (without nodules) obtained with a polypropylene grafted maleic anhydride compatibilizer. From these results and ours we suppose that stiffness improvement might not be

Table 5  
Stress at break ( $\sigma_b$ ), strain at break ( $\epsilon_b$ ), work at failure ( $W_b$ ) and relative work at failure ( $W_b/W_{b0}$ ) for DGEBA/D2000 based nanocomposites at 25 °C

DGEBA/D2000	$\sigma_b$ (MPa)	$\epsilon_b$ (%)	$W_b$ (kJ m <sup>-3</sup> )	$W_b/W_{b0}$
Neat	0.7	70	333	1
+5 phr Tixogel	1.2	120	807	2.42
+10 phr Tixogel	2.0	160	1713	5.14
+5 phr OPTC18	1.3	120	942	2.83
+5 phr Aerosil 200	1.3	120	774	2.32

Table 6  
Young’s modulus ( $E$ ), relative Young’s modulus ( $E/E_0$ ) and Poisson ratio ( $\nu$ ) for DGEBA/MCDEA based nanocomposites at 25 °C

DGEBA/MCDEA	$E$ (GPa)	$E/E_0$	$\nu$
Neat	2.67	1	0.31
+5 phr Tixogel	4.26	1.60	0.38
+5 phr OPTC18	2.80	1.05	0.40
+5 phr Aerosil 200	2.77	1.04	0.36

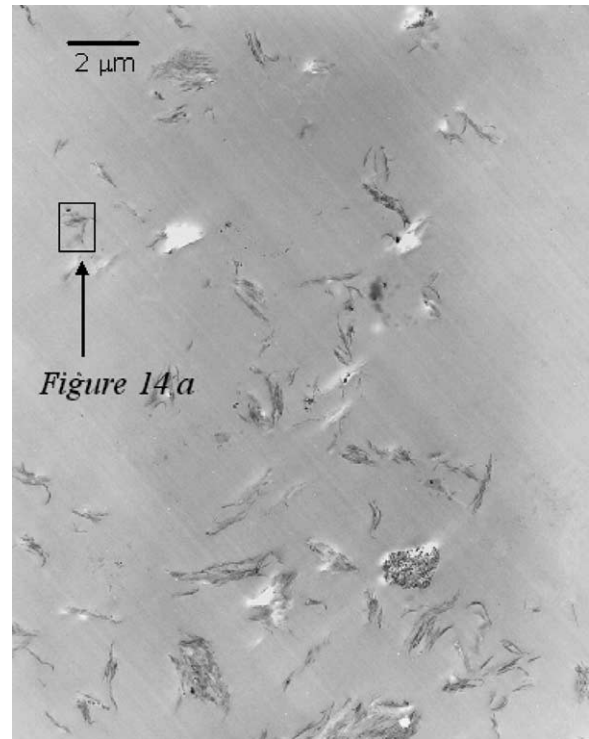


Fig. 12. TEM picture of DGEBA/MCDEA + 5 phr Tixogel composite.

directly linked to the state of dispersion at the nanometer scale level but that the whole state of dispersion for the micron to the nanometer has to be considered. In our case, when Figs. 12 and 13 are compared, we notice that the average aggregate size obtained with Tixogel is much smaller than with OPTC18, and that their aspect ratio is higher. This means that Tixogel, even if intercalated is homogeneously dispersed at a smaller scale level

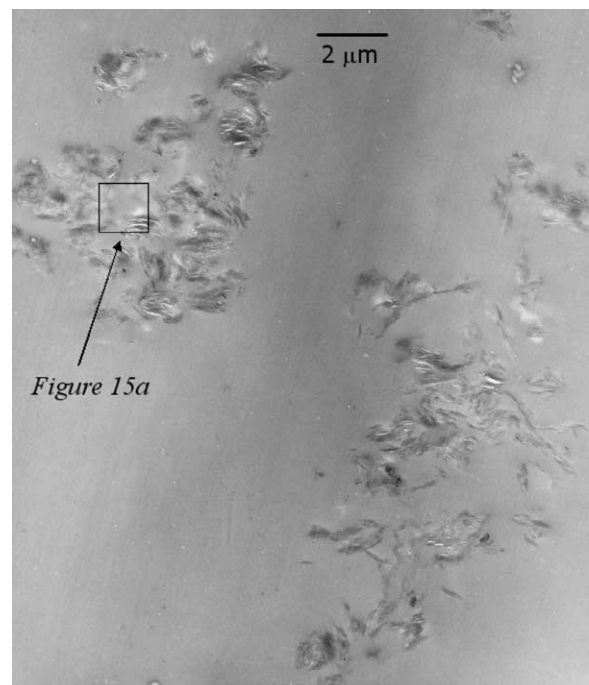


Fig. 13. TEM picture of DGEBA/MCDEA + 5 phr OPTC18 composite.

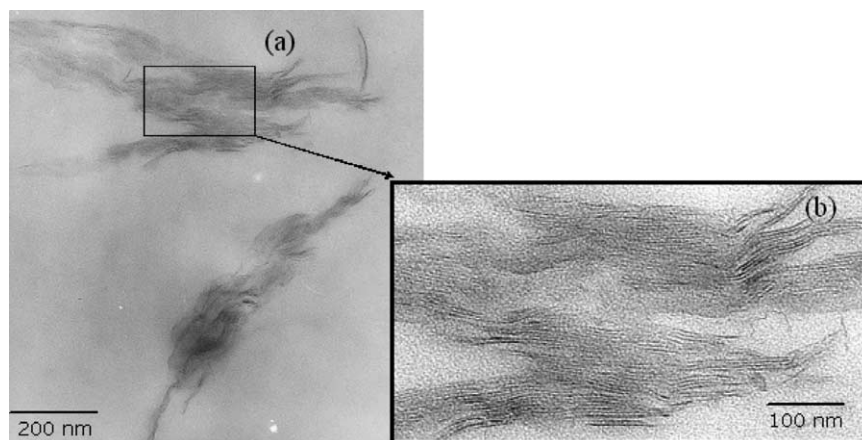


Fig. 14. TEM pictures of DGEBA/MCDEA + 5 phr Tixogel composite.

than OPTC18 and that its aggregates present an interesting aspect ratio. OPTC18 even if exfoliated at the nanometer scale forms big aggregates (no additional shear during processing of the composites) and is therefore, less homogeneously distributed in the matrix. This fundamental difference of morphology far above the nanometer scale might be responsible of the observed differences on the Young's modulus.

The measurements of the fracture toughness  $K_{Ic}$  of the DGEBA/MCDEA based nanocomposites (Table 7) reveal that improvements in stiffness and toughness of the thermoset matrix are not linked to the same kind of morphology.

Indeed, the toughness of the DGEBA/MCDEA glassy matrix is increased significantly (more than 40%) by both organoclays whereas conventional filler like silica does not give any significant improvement. The OPTC18 gives the best reinforcement (55%) whereas it did not allow increasing the modulus at all. These results are concordant with those of Miyagawa et al. [23], confirming that strong intercalated clay aggregates might induce crack deflection whereas fully

exfoliated platelets are easier to break. From the results we obtain with OPTC18, it seems that aggregates at the micrometer scale of exfoliated platelets can lead to very interesting reinforcements as well. The Tixogel, in spite of a poorer improvement in toughness, offers an interesting toughness/stiffness balance with low quantities of filler introduced and without optimizing the dispersion process.

This demonstrates that stiffness and toughness of nanocomposites are not linked to the same morphologies. Regarding the state of dispersion of Tixogel, it seems that stiffness is also dependant on the dispersion at the micrometer scale level. These results also demonstrate that organoclay can offer interesting improvements in mechanical properties of epoxy systems when compared to the one obtained using a conventional filler.

This study shows that the morphology of nanocomposites has to be considered at various scale levels if one aims at linking macroscopic properties to the state of dispersion and to the kind of alkylammonium ions used to modify montmorillonite.

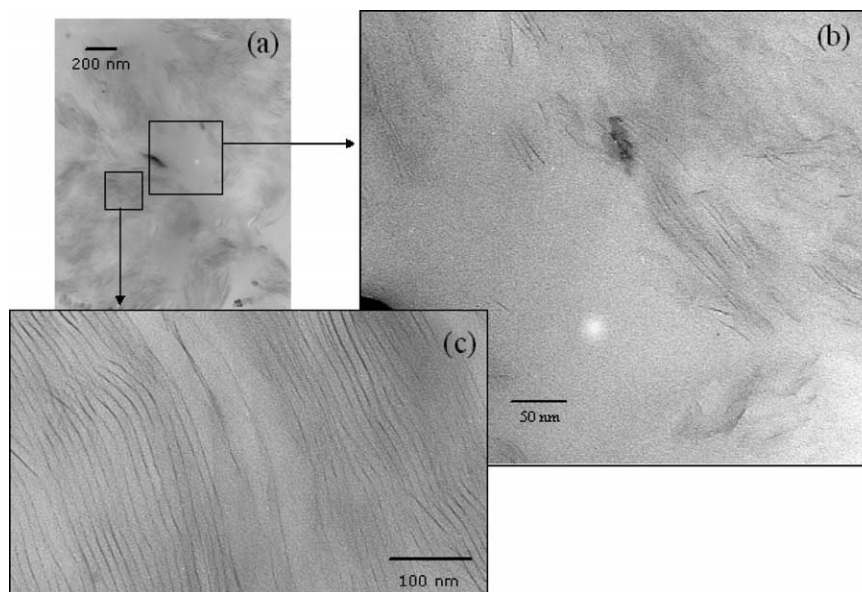


Fig. 15. TEM pictures of DGEBA/MCDEA + 5 phr OPTC18 composite.

Table 7  
Fracture toughness ( $K_{Ic}$ ) and relative fracture toughness ( $K_{Ic}/K_{Ic0}$ ) for DGEBA/MCDEA based nanocomposites at 25 °C

DGEBA/MCDEA	$K_{Ic}$ (MPa m <sup>1/2</sup> )	$K_{Ic}/K_{Ic0}$
Neat	0.75	1
+ 5 phr Tixogel	1.05	1.40
+ 5 phr OPTC18	1.16	1.55
+ 5 phr Aerosil 200	0.76	1.01

Finally it should be noted that the increase in the glassy modulus we obtained introducing 5 phr of Tixogel in the DGEBA/MCDEA system is much too high to be explained by any classical two phase mechanical model. The use of more complex models like the one proposed by Ji et al. [39] which take into account the interface volume fraction seems to be necessary.

#### 4. Conclusion

The morphologies obtained in epoxy/organoclay nanocomposites under study are intimately linked to the interactions between all the components of the initial unreacted suspension. We already demonstrated that an adequate compatibilisation of the montmorillonite leading to a consequent swelling of the galleries by the monomers was necessary to obtain intercalated or exfoliated nanocomposites [26]. We showed here that an additional increase in the interplatelet distance during the network polymerization and the amplitude of this increase are ruled by a complex competition between the polymerization and diffusion kinetics of the reactive mixtures as well as by the chemical nature of the alkylammonium ions at the montmorillonite surface.

In this study, the incorporation of organoclay to rubbery and glassy epoxy matrixes led to promising mechanical properties improvements even if we did not use any additional shear to disperse the clay (a previous study demonstrated its efficiency in improving the dispersion at the micrometer scale level [26]).

With the Tixogel organoclay we obtained an interesting stiffness/toughness balance for very low filler contents and without reducing the  $T_g$  of the matrix. This is particularly interesting when one thinks about how the brittleness of epoxies limits their use in technological areas where their high  $T_g$  is often highly appreciated.

#### Acknowledgements

We would like to thank Nathalie Issartel and Romain Bourdonnay for their help with mechanical properties characterization, Ruben Vera from Centre de Diffractométrie Henri Longchambon (UCB Lyon I) for performing XRD experiments and Mrs Rivoire from the Centre de microscopie

électronique appliqué à la biologie et la géologie (UCB Lyon I) for the TEM pictures.

#### References

- [1] Okada A, Kawasumi M, Usuki A, Kojima Y, Kurauchi T, Kamigaito O. *Mater Res Soc Proc* 1990;171:45–50.
- [2] Usuki A, Kojima Y, Kawasumi M. *J Mater Res* 1993;8(5):1179–84.
- [3] Pinnavaia TJ, Beal GW. *Polymer-clay nanocomposites*. New York: Wiley; 2001.
- [4] Kojima Y, Usuki A, Kawasumi M, Okada A, Fukushima Y, Kurauchi T, et al. *J Mater Res* 1993;8(5):1185–9.
- [5] Alexandre M, Dubois P, Sun T, Garces JM, Jerome R. *Polymer* 2002;43:2123–32.
- [6] Burgentzle D, Duchet J, Gerard JF, Jupin A, Fillon B. *J Colloid Interf Sci* 2004;278:26–39.
- [7] Moraru VN. *Appl Clay Sci* 2001;19:11–26.
- [8] Gherardi B, Tahani A, Levitz P, Bergaya F. *Appl Clay Sci* 1996;11:163–70.
- [9] Zilg C, Muelhaupt R, Finter J. *Macromol Chem Phys* 1999;200:661–70.
- [10] Vaia RA, Ishii H, Giannelis EP. *Chem Mater* 1993;5:1694–6.
- [11] Hackett E, Manias E, Giannelis EP. *J Chem Phys* 1998;108(17):7410–5.
- [12] Vaia RA, Tevkolsky RK, Giannelis EP. *Chem Mater* 1994;6:1017–22.
- [13] Pospisil M, Capcova P, Weiss Z, Malac Z, Simonik J. *J Colloid Interf Sci* 2001;245:126–32.
- [14] Lee A, Lichtenhan JD. *J Appl Polym Sci* 1999;73:1993–2001.
- [15] Kelly P, Akelah A, Qutubuddin S, Moet A. *J Mater Sci* 1994;29:2274–80.
- [16] Kornmann X, Lindberg H, Berglund LA. *Polymer* 2001;42:4493–9.
- [17] Lan T, Karivatna PD, Pinnavaia TJ. *ACS Polym Mater: Sci Eng* 1994;71:527–8.
- [18] Brown JM, Curliss D, Vaia RA. *Chem Mater* 2000;12:3376–84.
- [19] Becker O, Varley R, Simon G. *Polymer* 2002;43(16):4365–73.
- [20] Messersmith PB, Giannelis EP. *Chem Mater* 1994;6(10):1719–25.
- [21] Zerda AS, Leser AJ. *J Polym Sci, Part B: Polym Phys* 2001;39:1137–46.
- [22] Zilg C, Muelhaupt R, Finter J. *Macromol Chem Phys* 1999;200:661–70.
- [23] Miyagawa H, Drzal LT. *J Adhesion Sci Technol* 2004;18(13):1571–88.
- [24] Lan T, Karivatna PD, Pinnavaia TJ. *Chem Mater* 1995;7:2144–50.
- [25] Chen JS, Poliks MD, Ober CK, Zhang Y, Wiesner U, Giannelis EP. *Polymer* 2002;43(18):4895–904.
- [26] Le Pluart L, Duchet J, Sautereau H, Halley P, Gerard JF. *Appl Clay Sci* 2004;25(3–4):207–19.
- [27] Girard-Reydet E, Riccardi CC, Sautereau H, Pascault JP. *Macromolecules* 1995;28:7599–607.
- [28] Winter H, Chambon F. *J Rheol* 1986;30:367–82.
- [29] Chambon F, Winter HH. *J Rheol* 1987;31:683–97.
- [30] Pascault JP, Williams RJJ. *J Polym Sci, Polym Phys* 1990;28:85–95.
- [31] Verchere D, Sautereau H, Pascault JP, Riccardi CC, Maschiar SM, Williams RJJ. *Macromolecules* 1990;23:725–31.
- [32] Williams JG, Cawood MJ. *Polym Test* 1990;9:15–26.
- [33] Wang MS, Pinnavaia TJ. *Chem Mater* 1994;6:468–74.
- [34] Miller DR, Macosko CR. *Macromolecules* 1976;9(2):206–11.
- [35] Pascault JP, Sautereau H, Verdu J, Williams RJJ. *Thermosetting polymers*. New York: Marcel Dekker; 2002.
- [36] Eloundou JP, Feve M, Gerard JF, Harran D, Pascault JP. *Macromolecules* 1996;29:6907–16.
- [37] Le Pluart L, Duchet J, Sautereau H, Gerard JF. *J Adhesion* 2002;78:645–62.
- [38] Boucard S, Duchet J, Gerard JF, Prele P, Gonzalez S. *Macromol Symp* 2002;194(1):241–6.
- [39] Ji XL, Jing JK, Jiang W, Jiang BZ. *Polym Eng Sci* 2002;42(5):983–93.